Histomorphological and histomorphometric analysis of wollastonite and tricalcium phosphate composite at different concentrations after in vivo implantation

Análise histomorfológica e histomorfométrica do compósito wollastonita e fosfato tricálcico em diferentes concentrações após implantação in vivo

DOI:10.34117/bjdv9n1-363

Recebimento dos originais: 23/12/2022
Aceitação para publicação: 26/01/2023

Luisa Queiroz Vasconcelos
PhD in Interactive Processes of Organs and Systems by Universidade Federal da Bahia (UFBA)
Institution: Universidade Federal da Bahia - Instituto de Ciencias da Saude, Salvador, Bahia
Address: Av. Reitor Miguel Calmon, S/N, CEP: 40110-100, Salvador - BA, Brasil
E-mail: luisa-queiroz@hotmail.com

Mauricio Mitsuo Monção
PhD in Interactive Processes of Organs and Systems by Universidade Federal da Bahia (UFBA)
Institution: Universidade Federal da Bahia - Instituto de Ciencias da Saude, Salvador, Bahia
Address: Av. Reitor Miguel Calmon, S/N, CEP: 40110-100, Salvador - BA, Brasil
E-mail: maurimitsuo@yahoo.com.br

Aryon de Almeida Barbosa Júnior
PhD in Medicine by Universitat Zu Bonn Rheinischen Friedrich Wilhems (UNI – BONN) - Alemanha
Institution: Fundacao Oswaldo Cruz, Instituto Gonçalo Moniz, Salvador - BA
Address: R. Waldemar Falcão, 121, Candeal, Salvador - BA, CEP: 40296-710
E-mail: ary3on@hotmail.com

Raúl Garcia Carrodeguas
PhD in Chemical Sciences by Universidade da Havana
Institution: Universidade Federal de Campina Grande, Campina Grande - PB
Address: Rua Aprígio Veloso, de 748/749 ao fim Universitário, Campina Grande – PB, Brasil
E-mail: rgcarrodeguas@gmail.com

Isabela Cerqueira Barreto
PhD in Interactive Processes of Organs and Systems by Universidade Federal da Bahia (UFBA)
Institution: Universidade Federal da Bahia - Instituto de Ciencias da Saude, Salvador, Bahia
Address: Av. Reitor Miguel Calmon, S/N, CEP: 40110-100, Salvador - BA, Brasil
E-mail: isabela.barreto@ufba.br

Roberto Paulo Correia de Araújo
Doctorate in Dentistry by Universidade Federal da Bahia (UFBA)
Institution: Universidade Federal da Bahia Instituto de Ciencias da Saúde, Salvador, Bahia
Address: Avenida Reitor Miguel Calmon, S/N, Vale do Canela, Canela, CEP: 40110-902, Salvador, BA - Brasil
E-mail: rpcaraujo@hotmail.com

ABSTRACT
Purpose: To evaluate, through histomorphometric analysis in critical bone defect, the osteogenic behavior of new glass-ceramic biomaterials in granules, named different from pseudowollastonite (p-W) and beta tricalcium phosphate (β-TCP). Methods: Forty Wistar rats were randomly distributed into 4 groups, with 5 animals in each group recovered at 15 and 45 days: G20/80 (20% p-wollastonite and 80% β-tricalcium phosphate); G60/40 (60% p-W and 40% β-TCP); G80/20 (80% p-W and 20% β-TCP); and CG (control group). Results: A histomorphological analysis showed that, in all rules, the composites were biocompatible and bioactive. The G60/40 presents osteoid matrix deposition in 65% of the bone defect at 45 days. While the other groups formed similar percentages of bone neoformation in both biological points. Conclusion: The studied composites are biocompatible, fillers and osteoconductive.

Keywords: biocompatible materials, calcium silicate, calcium phosphate, bone regeneration.

RESUMO
Objetivo: Avaliar, através da análise histomorfométrica em defeitos ósseos críticos, o comportamento osteogênico de novos biomateriais vitrocerâmicos em grânulos, denominados diferentes da pseudowollastonita (p-W) e do fosfato tricálcico beta (β-TCP). Métodos: Quarenta ratos Wistar foram distribuídos aleatoriamente em 4 grupos, com 5 animais em cada grupo recuperados aos 15 e 45 dias: G20/80 (20% p-wollastonite e 80% β-tricalcium phosphate); G60/40 (60% p-W e 40% β-TCP); G80/20 (80% p-W e 20% β-TCP); e CG (grupo de controle). Resultados: Uma análise histomorfológica mostrou que, em todas as regras, os compósitos eram biocompatíveis e bioativos. O G60/40 apresenta deposição de matriz osteóide em 65% do defeito ósseo aos 45 dias. Enquanto os outros grupos formavam porcentagens semelhantes de neoformação óssea em ambos os pontos biológicos. Conclusão: Os compósitos estudados são biocompatíveis, preenchedores e osteocondutivos.

Palavras-chave: materiais biocompatíveis, silicato de cálcio, fosfato de cálcio, regeneração óssea.

1 INTRODUCTION

The use of biomaterials in dentistry and medicine has been an ally to restore health, function and aesthetics in areas with great bone loss. Bone substitutes, defined as biomaterials, of natural or synthetic origin, are intended to interact with biological systems, either transiently or permanently, with the aim of filling or replacing biological tissues or organs[1,2]. For this, it is necessary to understand biological responses, from the physical, mechanical and chemical properties of these biomaterials. Tissue bioengineering uses knowledge from biological sciences and engineering to develop new technologies and tissue substitutes[1].

Bone lesions of critical dimensions are characterized by compromised blood supply and cells, due to the absence of a framework that helps in the repair of this tissue. In this condition, the repair takes place by deposition of fibrous connective tissue, which does not provide structural organization to the tissue, making it necessary to implant a framework that guides the migration of cells and osteogenic factors so that the deposition of new bone tissue occurs[3]. Given this need, biomaterials can be a therapeutic option since they are produced with a composition or architecture similar to that of bone tissue. In addition, they have good availability, easy sterilization and are less likely to cause morbidity. For the use of these materials as bone substitutes to be viable, there must be biocompatibility, osteoconduction and biodegradation[1,3].

Tricalcium phosphate (TCP) and wollastonite (W) have been standing out among the different types of biomaterials. TCP is a non-immunogenic, biodegradable, biocompatible and osteoconductive ceramic, as it guides osteoblasts in bone neoformation. W is a bioactive calcium silicate that promotes improvements in the biomechanical properties of calcium phosphates due to the high degradability and bioactivity inherent to its properties. The silicon present in W is related to greater osteogenesis due to its participation in important physiological processes, such as the osteoblast cell cycle[3,4,5].

The strategy of associating W with TCP, in different concentrations, allows the development of a bioceramic with soluble capacity in biological medium and gradual release of calcium, phosphate and silicon ions, stimulating the formation of new bone tissue. This framework should contribute to cellular implantation, migration and proliferation, which are essential for tissue regeneration. Therefore, the innovation of this study was to use a new composite based on the polymorphous pseudowollastonite (p-W),

bioactive and biodegradable calcium silicate and beta tricalcium phosphate (β-TCP), the most stable phase of tricalcium and bioresorbable phosphates, at different concentrations, which allowed analyzing the tissue response and the behavior of p-W/β-TCP composite after implantation in a critical bone defect for application in bone tissue therapy.

2 MATERIALS AND METHOD

This study was approved by the Ethics Committee on Research in the Use of Animals, of the Institute of Health Sciences of the Federal University of Bahia (protocol 128/2017) and followed the Ethical Standards for Research in Animals (Law No. 11,794). 2008), as well as the National Biosafety Standards and the National Institute of Health guidelines for the care and use of laboratory animals (NIH Publication No. 85-23, ver. 1985).

2.1 BIOMATERIAL

The biomaterial (G80/20, G60/40 and G20/80) were prepared, characterized and supplied by the Institute of Ceramics and Glass (ICV-CSIC, Madrid, Spain). The compositions of the biomaterials were chosen to obtain different degrees of bioabsorption, one that ρ-W is more soluble and bioactive than β-TCP in physiological fluids[4]. During the preparation of the biomaterial natural wollastonite, $CaSiO_3$ (NYCO, NYAD M1250, Batch Number M1404227J01), whose molar composition was 52.94% of SiO_2 and 44.94% of CaO and tricalcium phosphate, $Ca_3(PO_4)_2$ (Sigma-Aldrich, Ref. 21218, lot number BCBM7330V) in different amounts, depending on the desired W and TCP concentration, as shown in Table 1. After weighing the specific amounts of raw materials for each concentration, the composites were ground with the aid of zirconia beads 3.0 mm in diameter in the attrition mill for 15 minutes and isopropyl was added. The composites were dried at 60 °C for 24 h. After drying, the materials were sintered at 1250 °C, at different times, depending on the concentration (Table I). The temperature was chosen based on the study by Almeida (2017)[1]. In which this author performed previous dilatometric studies, which indicated a maximum densification rate for the three experimental compositions around 1250 °C. This temperature falls within the binary field of the phase equilibrium diagram of the W-TCP system[6]. Different times were used for each composition to allow sintering and, at the same time, to avoid the excessive formation of glass, which is formed through local melts in greater quantity in the

compositions richer in W. After sintering, the composites underwent a grinding process with the aid of a jaw crusher, which allowed a new granulometry in the range of 0.6 - 0.4 mm.

Table 1 - Chemical composition of composites at different concentrations and temperatures used to obtain them.

Biomaterials	**Quantity (MP)**		**Expected chemical composition (%m/m)**				**Sintering conditions**	
Concentration p-W/ β-TCP	W (g)	TCP (g)	CaO	SiO_2	P_2O_5	Others	T (°C)	T (min)
80/20	80,0	20,0	51,34	10,61	35,72	2,33	1250	5
60/40	60,0	40,0	48,25	31,87	17,89	1,99	1250	60
20/80	20,0	80,0	46,70	42,52	8,85	1,93	1250	180

2.2 CHARACTERIZATION OF BIOMATERIALS

The samples were analyzed by scanning electron microscopy (SEM) at the Materials Characterization Laboratory (LCM), of the Federal Institute of Education, Science and Technology of Bahia (Salvador - Brazil), to obtain microphotographs for better understanding of the superficial aspects through the quantitative analysis of the particles and pores of the groups. The samples were placed on a double-sided carbon tape, fixed in a smooth-surfaced sample holder and inserted into a metallizer (Quorum Technologies, model Q150R). The ionic deposition parameters established were as follows: ambient temperature at 25°C, current of 20 mA, voltage of 2 kV and deposition time of 120 seconds, providing a gold film on the surface of the particles in the order of 25 nm. To obtain the micrographs, the present study used a TESCAN scanning electron microscope, model VEGA 3 LMU, by the secondary electron method, with a working distance of 15 mm and electron acceleration voltage of 10 kV. Micrographs were obtained with different increases in SEM.

2.3 IN VIVO ASSAY

Forty adult male albino Wistar rats, with body weight between 350 and 400g, were randomly distributed into eight experimental groups, with five animals in each: G20/80 – critical bone defect filled with granules 20% p-W and 80% β-TCP; G60/40 – critical bone defect filled with granules 60% p-W and 40% β-TCP; G80/20 – critical bone defect filled with granules of 80% p-W and 20% β-TCP ; GC – critical bone defect filled with clot. The groups were evaluated at the biological points of 15 and 45 days. During the entire experiment, the animals were kept in individual plastic boxes, identified according

to the experimental group and the biological point; and received food and water ad libitum.

The animals were anesthetized with intraperitoneal injection of xylazine hydrochloride (0.06 ml/kg) and ketamine hydrochloride (0.12 ml/kg). After anesthesia, trichotomy and antisepsis of the calvaria region with iodized alcohol were performed. Subsequently, a critical bone defect of approximately 8.0 mm in diameter was made in the medial portion of the calvaria with a trephine bur. This defect was filled according to the pre-established experimental groups mentioned in the previous step. Upon reaching the biological point of 15 and 45 days, the animals were euthanized by deepening anesthesia, according to Normative Resolution No. 37/2018 of the National Council for the Control of Animal Experiments (CONCEA). The specimens were fixed for 72 h in 4% buffered formaldehyde (Aldrich, United Kingdom), sectioned in half, obtaining the anterior and posterior portions. The posterior portion was decalcified with 5% EDTA (Aldrich, UK) for 7 days and then embedded in paraffin. The anterior portion remained in formalin to be embedded in resin. Each specimen was cut to 5.0 µm thick and stained with hematoxylin-eosin (HE) and picrosirius-red (PIFG) for histological analysis by light microscopy. Histomorphometric analysis was performed by optical microscopy using a MM6B microscope coupled to a DFC7000T digital camera and the LAS Core image processing analysis system (Leica, Germany).

2.4 MORPHOMETRIC AND STATISTICAL ANALYSIS

The Leica Application Suite (LAS) v. software was used for the histomorphometric analysis. 4.12 (Leica®) to quantify the linear fill (mm) and area (mm^2) of new bone formation of the critical bone defect. To compare the differences between the experimental groups, fixing the biological point and testing different groups, the non-parametric Kruskal-Wallis test (between three groups) and the Mann-Whitney test (between two groups) were used. To compare the differences between the experimental groups by fixing the group and testing different biological points, the non-parametric Wilcoxon Signed Ranks test was used. Analyzes were performed using IBM SPSS Statistics v. 20 for Windows 2010, with a significance level of 5% ($p < 0.05$).

3 RESULTS

In the SEM analysis image, it is possible to observe that the granules are irregular, multiple, faceted and angular. Furthermore, the surface aspects of the granules are similar in the three concentrations, containing pores (Figure 1).

Figure 1 – Photomicrographs of the surface of the granules by SEM at concentrations 20/80 (B-D), 60/40 (F-H) and 80/20 (J-L) of the granule samples of the biomaterial composed of W and β-TCP. Micrographs of granules at concentrations 20/80 (A), 60/40 (E) and 80/20 (I) show solid, varied and random forms.

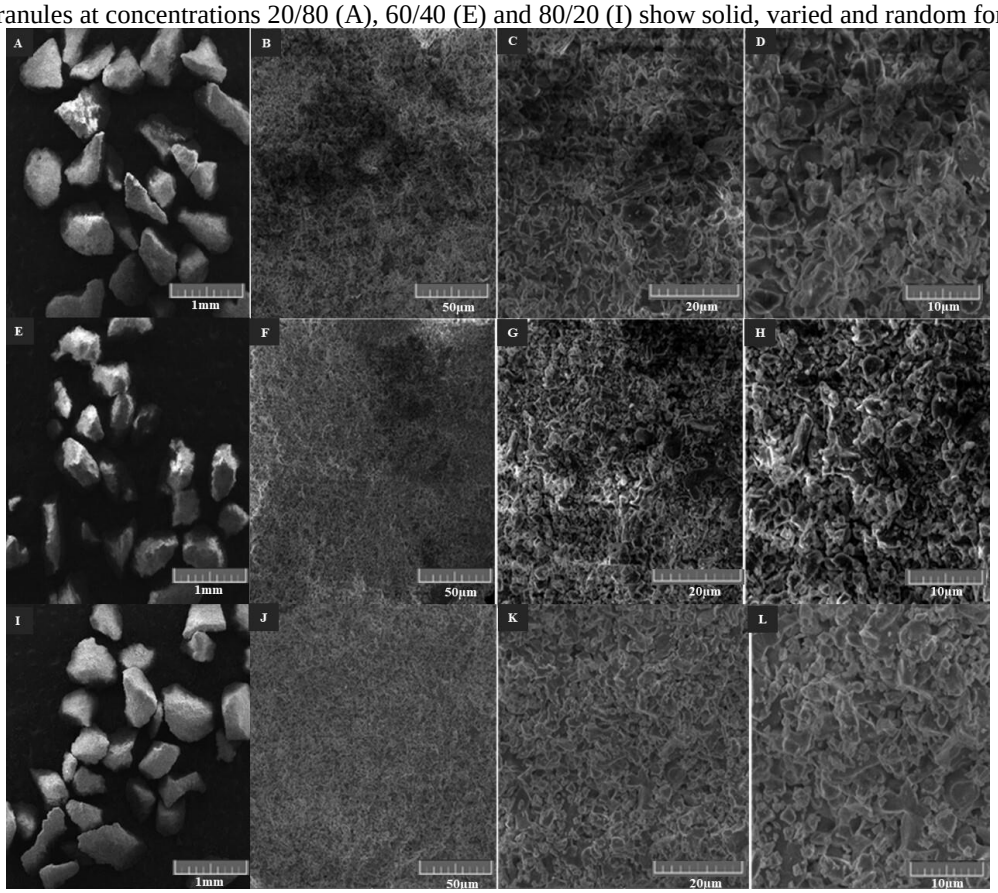

In the histological analysis of the group G20/80 at 15 and 45 days, it was possible to observe the reactive osteoid matrix at the edges of the defect with a thickness proportional to the bone edge and with the presence of osteocytes (Figure 2). In both biological points, there was no deposition of osteoid matrix in the center of the defect, but deposition of newly formed connective tissue surrounding the biomaterial, blood vessels and the presence of multinucleated giant cells (Figure 2, V-VIII). The granules were found to be more biodegradable at 45 days than at 15 days postoperatively (Figures 1), with the presence of acute and chronic granulomatous inflammation around them (Figures 2, I, III, V and VII).

In both biological points, the presence of septa was observed inside the biomaterial (Figure 2). At 15 and 45 days, the defect was filled by the biomaterial to the full extent in multiple layers (Figure 3). At 45 days, the presence of mesenchymal cells was observed in the interstitium of the granules. The deposition of collagen fibers occurred in denser and more organized concentric layers on the periphery of the granules; in the center of the granules, collagen fibers with loose organization (Figure 2). It was possible to visualize, at 15 and 45 days, inflammatory cells with emphasis on the giant cells around and inside the granules (Figure 2).

Figure 2 – Photomicrograph of the filling of the defect by granules in the G20/80 groups throughout the experiment represent the 15-day biological the 45-day biological point. Photomicrographs obtained from the edge and center of the defect at 15 and 45 days of implantation of biomaterials in G20/80. Bone rim (BE), osteoid matrix (OM), granule (GR), central vein (VC), dura mater region (DM), loose connective tissue (LCT), blood vessel (*), multinucleated giant cell (head arrow), osteocytes (black arrow). Staining: HE.

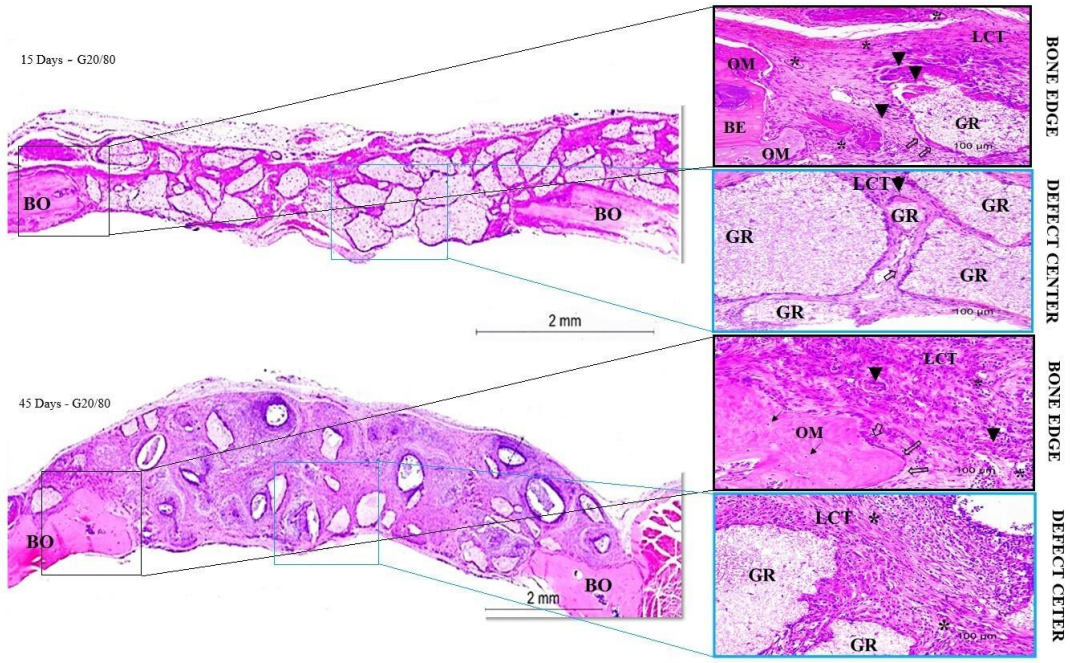

In the histological analysis of the group G60/40 at the biological point of 15 days, deposition of a reactional osteoid matrix was observed, starting from the edges of the bone defect and in a centripetal direction (Figure 3). At 45 days, osteoid matrix deposition was noted beyond the bone edges in the central region of the defect, surrounding it and inside the biomaterial particles, filling the entire defect (Figures 3). It is possible to distinguish regions, at 45 days of osteoid matrix with a more organized and denser characteristic of the immature matrix. In addition, bone marrow formation was observed along the entire linear extension of the defect (Figure 3). Both at 15 and 45 days, the

granules occupied the entire length of the defect, arranged in multiple layers (Figure 3), with different sizes and with a slightly basophilic appearance, reticulated in the center and sometimes surrounded by osteoblasts (Figures 3). At 45 days, it was noted that the granules had a smaller diameter and were replaced either by connective tissue or by osteoid matrix compared to 15 days.

Figure 3 – Photomicrograph of the filling of the defect by granules in the G60/40 groups throughout the experiment represent the 15-day biological the 45-day biological point. Photomicrographs obtained from the edge and center of the defect at 15 and 45 days after implantation of biomaterials in G60/40. Bone rim (BE), Osteoid matrix (OM), granule (GR), central vein (VC), dura mater region (DM), loose connective tissue (LCT), blood vessel (*), multinucleated giant cell (head arrow), osteocytes (black arrow). Staining: HE.

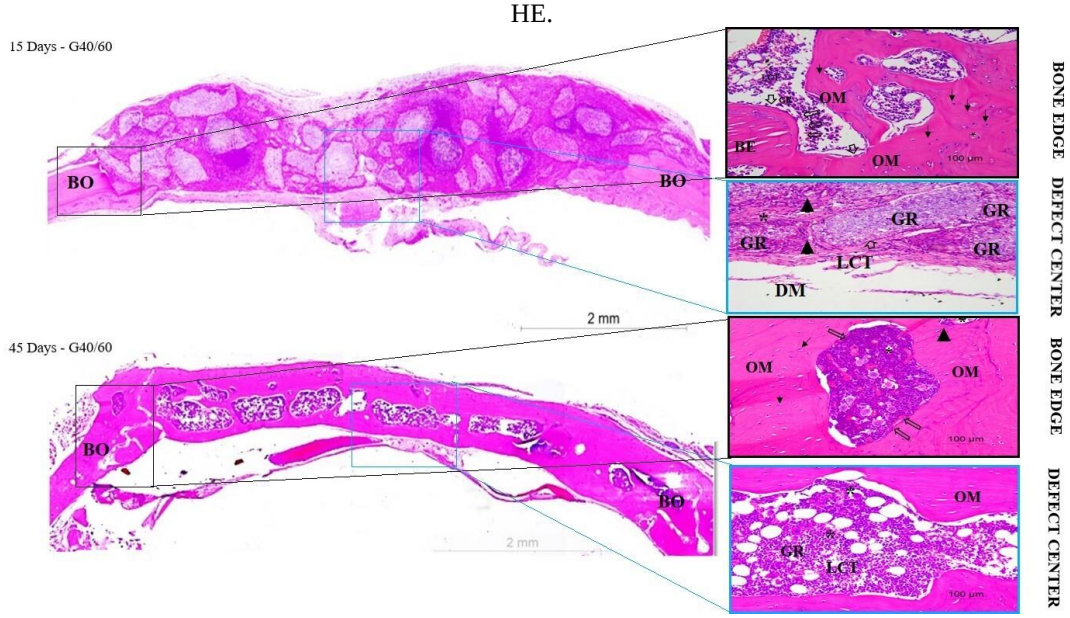

In the histological analysis of the group G80/20 at 15 and 45 days, a discrete formation of reactive osteoid matrix was observed at the edges of the defect (Figures 4). However, it was possible to observe the filling of the entire defect by multiple layers of granules and in different sizes (Figure 4). Adjacent to the granules, there was a chronic inflammatory reaction of the granulomatous type, accentuated with the presence of macrophages and giant cells (Figures 4). At 45 days, fine septa of collagen fibers were observed permeating and penetrating the granules in a centripetal direction, with denser collagen fibers, organized in parallel layers and with loose connective tissue among the collagen fibers (Figure 4). At 45 days, there was formation of blood vessels connecting the granules and it was possible to observe small areas of osteoid matrix in the most peripheral regions of the defect, with the presence of osteocytes (Figure 4).

Figure 4 – Photomicrograph of the filling of the defect by granules in the G80/20 groups throughout the experiment represent the 15-day biological the 45-day biological point. Photomicrographs obtained from the edge and center of the defect at 15 and 45 days of implantation of biomaterials in G80/20. Bone rim (BE), Osteoid matrix (OM), granule (GR), central vein (VC), dura mater region (DM), loose connective tissue (LCT), blood vessel (*), multinucleated giant cell (head arrow), osteocytes (black arrow). Staining: HE.

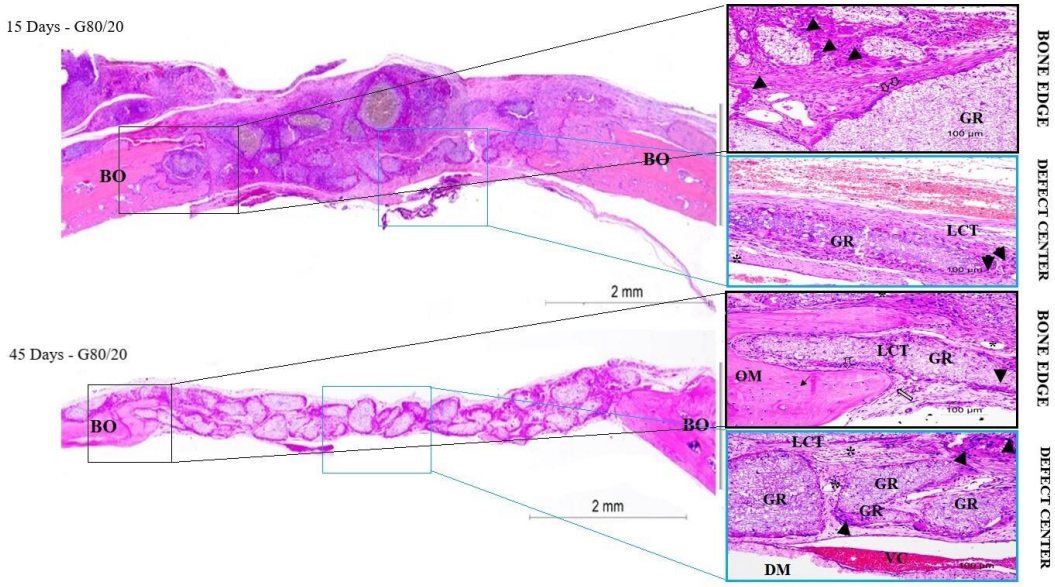

The histomorphometric and statistical analysis of the G60/40 at 45 days showed 65.25% of filled area and 100% of linear extension of the critical bone defect with deposition of neoformed osteoid matrix (Wilcoxon Test p= p=0.109). However, the analysis of the filled area and the analysis of linear extension by neoformed osteoid matrix between groups showed no statistically significant difference between the means of the groups (Mann-Whitney p = 0.044).

4 DISCUSSION

Autogenous grafts are an excellent option for a bone substitute, as they are osteoconductive and osteoinductive. However, for the use of this type of graft, an additional surgical procedure is necessary in the tissue donor region and, often, the amount of bone acquired is insufficient. Therefore, an option for cases that require a bone substitute is the biomaterial. The alloplastic graft needs to have adequate properties, chemical composition and degradation; be non-toxic, have biodegradability, be effective. It should also provide mechanical support for cell colonization, stimulate migration, adhesion and differentiation of osteoprogenitor cells and favor angiogenesis[5]. Therefore, the objective of this study was to evaluate the osteogenic behavior of a new composite

consisting of different concentrations of p-W and β-TCP as a therapeutic option for bone grafting.

The experimental model of critical bone defect in rats was used, because, since the bone lesion has critical morphology and dimensions, associated with vascularization deficiency, an alternative and complementary therapy is necessary to guarantee bone regeneration. Among the different materials used in recent decades, biomaterials with association of W with polymorphs of TCP have been developed so that there is a better understanding of the biological function (biocompatibility, osteogenesis, osteoinduction and osteoconduction) required to be used as bone grafts[1,4,6].

The biomaterial studied (p-W/β-TCP) showed to be surrounded by granulomatous reaction in all groups, at concentrations 20/80, 60/40 and 80/20 at 15 days post implantation. When implanting a biomaterial, a local inflammatory response is expected, due to the rupture of blood vessels as a result of tissue injury and the presence of the material in contact with body fluids[2,3,6]. Thus, the biomaterial studied was biocompatible.

The formation of fibrous septa and the presence of inflammatory cells in the inner portion of the granules as giant cells corroborate the study carried out by Furusawa et al. (1998)[8] in rats treated with Biogran® (bioactive glass, Orthovita, Malvern, PA), as it was observed that, within a week of repair, there were osteogenitor cells in the fissures of the biomaterial granules. In the third week, they observed that the center of the granules was filled with osteogenic cells and, after 4 weeks, there was resorption of the center of the granule, phagocytosis and formation of osteoid matrix.

In our study, it was observed, at 15 and 45 days, that the size and shape of the granules, in both groups of the pW/β-TCP composite, in the bone defect, allowed their disposition, mostly, in multiple layers, with formation of interconnections and porosity, which contributed to neoangiogenesis at an early and later stage of repair. The deposition of osteoid matrix was concentrated only on the edges of the defect, at concentrations of G20/80 and G80/20, in both biological points. However, the G60/40 group presented osteoid matrix deposition on the edges and along the entire bone defect, including the center. Coathup et al. (2018)[9] report that there is no consensus in studies focusing on bone regeneration on an ideal level of porosity formed by biomaterials that promotes cell migration and fixation. In another study, Fetner et al. (1994)[10] used bioglass (PerioGlas®) with different granulometries (90-310 µm and 500-710 µm) for bone

regeneration through a defect performed in the mandible of a monkey and the results did not reveal any difference. in the repair process between the materials.

However, in the 90's, Grégoire, Orly and Mentanteau[11] already correlated the particle size of the biomaterial as a relevant factor in the phagocytosis process and, consequently, in a better bioactivity and better adhesion of bone cells. For, after the phagocytosis of the particles, there is an increase in gene transcription and protein biosynthesis, which is characterized by a greater metabolic activity. The pore size must be between 100 and 300 μm. In this size range, proliferation of capillaries occurs to supply the metabolic needs of cells and cellular accommodation of bone tissue. The characterization of the granules through morphological analysis using a scanning electron microscope demonstrates that the shape of both composites is quite different. Wollastonite has an acicular shape and β-TCP is smaller in size than wollastonite. The heterogeneity in the shape of the granules favors the formation of a framework with different pore sizes. Pores smaller than 75-100 μm result in the growth of non-mineralized osteoid tissue. Furthermore, pores smaller than 5 μm allow neovascularization and fibroblast growth of 5 to 15 μm[2,5,8].

The composite used in this study had the shape of a granule, which already provides a distribution and the formation of a framework with spaces between granules of different sizes and shapes. Such a feature presented in this format will influence the conduction of cells and, consequently, the tissue response to osteoid matrix deposition. It is noted that, in the different concentrations studied of the p-W and β-TCP composite, at 15 days, there was no deposition of osteoid matrix beyond the edges. However, at 45 days, it is possible to observe deposition of osteoid matrix beyond the edges of the bone defect at G20/80 and G80/20 groups; at the G60/40 group there was production of osteoid matrix throughout the entire length. The findings observed in the histology show that this granule-shaped composite provided osteoconduction of cells and growth factors.

Another physical characteristic of the composite studied that may have influenced the small production of osteoid matrix at 15 days is the size of the surface area of the particles available to react with cells and biological fluid. The larger the particle size, the longer the biomaterial reabsorption time. Such an aspect may have resulted in a total repair of the defect by a fibrous connective tissue, at 15 days. These findings are consistent with the work developed by Almeida (2013)[12] during the evaluation of the biocompatibility and biofunctionality of 2-TCP and 2-TCP/bioglass granules. During

sintering, particles approach, leading to volumetric contraction of the material. At the end of the process, there is a significant reduction in its specific surface area, causing the system to reach a condition of lower free energy. This reduction in surface area also leads to a decrease in the bioactivity of the glass. The granules filled the entire bone defect, in both studied groups, with a reticular appearance, suggestive of a degradation process, at 15 days. The appearance of the granules described above is related to the high solubility of p-W and β-TCP. Some granules presented fibrous septa in the middle of the degradation process. This may have occurred because the surface of this composite has high porosity, which increases the surface reactivity of the biomaterial in the interstice[6,7,12,13].

It is observed that the granules, in the G20/80 and G80/20 groups, at 45 days postoperatively, have a large amount of internal septa, with the presence of inflammatory cells, including giant cells, with an intense aspect of degradability and deposition of concentric collagen fibers around the granules. In the G60/40 group, at 45 days postoperatively, it was observed that granules were replaced by osteoid matrix. Even forming a framework dependent on the distribution of granules, the chemical properties inherent to the different composites studied show that the proportion of wollastonite and TCP influences the pattern of biological response. Or it may have provided similar neoformation rates between the G20/80 and G80/20 groups, when compared to the G60/40 group, due to the physicochemical characteristic of the ρ-W/β-TCP composite, since the processes of Sintering increases crystallization, which favors crystal fusion and growth particle aggregation, making them resistant to biodegradation. This reduces the transfer of ions and the reactivity of the material becomes lower[12,14,15,16].

5 CONCLUSION

The biomaterial based on p-W and β-TCP (p-W/β-TCP) at concentrations of 20/80, 60/40 and 80/20, were considered biocompatible and bioactive. At 45 days, G60/40 completely filled the bone defect with neoformed osteoid matrix in thickness and height of the bone edge. The framework formed by the distribution of granules favored migration and adhesion of fibroblasts along the entire length of the bone defect and in all groups and biological points studied.

REFERENCES

1. Guastaldi AC, Aparecida AH. Fosfato de cálcio de interesse biológico: importância como biomateriais, propriedades e métodos de obtenção de recobrimento. Quim Nova, 2010;33(6):1352-13528.

2. Miguel FB, Cardoso AKMV, Barbosa Junior AA, Elcio Marcantonio Junior E, Goissis G, Rosa FP. Morphological assessment of the behavior of three dimension alanionic collagen matrices in bone regeneration in rats. J BiomedMater Res. 2006;78(2):334-339. https://doi.org/10.1002/jbm.b.30492

3. Carrodeguas RG, De Aza PN, De Aza. Main contributions to bioceramics. Boletin de la Sociedad Espanola de Ceramica y Vidrio. 2011;50(6):301-309. https://doi.org/10.3989/cyv.292011

4. Tedeja A, Piña C, Martínez S, Avila G. Cerámicas bioeutecticas W-TCP. Revista Mexicana de Física. 2004;50(2):187-192.

5. Barbosa WT, De Almeida KV, De Lima GG, Rodriguez MA, Lia Fook MV, Carrodeguas RG, et al. Synthesis and in vivo evaluation of a scaffold containing wollastonite/β-TCP for bone repair in a rabbit tibial defect model. J Biomed Mater Res B Appl Biomater. 2019;8:1-10. https://doi.org/10.1002/jbm.b.34462.

6. Artas G, Gul M, Acikan I, Kirtay M, Bozoglan A, Simsek S, et al. A comparison of different bone graft materials in peri-implant guided bone regeneration. Braz. oral res. 2019;13:32-59. https://doi.org/10.1590/1807-3107bor-2018.vol32.0059.

7. Gaspar AMM, Saska S, Carrodeguas RG, De Aza AH, Péna P, De Aza PN, et al. Biological response to wollastonite doped α-tricalcium phosphate implants in hard and soft tissues in rats. Key Engineering Materials. 2009;396:7-10. https://doi.org/10.4028/www.scientific.net/KEM.396-398.7

8. Furusawa T, Mizunuma K, Yamashita S, Takahashi T. Investigation of early bone formation using resorbable bioactive glass in the rat mandible. Int J Oral and Maxillofac Implants. 1998;13(5):672-676.

9. Coathup MJ, Hing KA, Samizadeh S, Chan O, Fang YS, Campion C, et al. Effect of increased strut porosity of calcium phosphate boné graft substitute biomaterials on osteoinduction. Journal of Biomedical Materials Research Part A. 2012;100A(6):1550-1555. https://doi.org/10.1002/jbm.a.34094.

10. Fetner AE, Hartigan M, Low SB. Periodontal repair using Perioglass in nonhuman primates: clinical and histologic observations. Compend Cont Educ Dent. 1994;5:932-938.

11. Grégoire M, Orly I, Menanteau, J. The influence of calcium phosphate biomaterials on human bone cell activities. An in vitro approach. Journal of Biomedical Materials Research. 1990;24(2):165-177. https://doi.org/10.1002/jbm.820240204

12. Almeida RS. Avaliação da implantação de grânulos de ²-TCP associado ou não à biovidro fosfatado para regeneração de defeito ósseo [dissertação]. Instituto de Ciências da Saúde, Universidade Federal da Bahia, 2013.

13. Pérez RA, Won J-E, Knowles JC, Kim HW. Naturally and synthetic smart composite biomaterials for tissue regeneration. Advanced drug delivery reviews. 2013;65(4):471–496. https://doi.org/10.1016/j.addr.2012.03.009

14. Santos GG, Vasconcelos LQ, Poy SCS, Almeida RdosS, Barbosa Júnior AA, Santos SRdeA, et al. Influence of the geometry of nanostructure dhydroxyapatiteand alginate composites in the initial phase of bone repair. Acta Cir. Bras. 2019;34(2):201900203. https://doi.org/10.1590/s0102-8650201900203

15. Alimi M, Navarro-Ramirez R, Parikh K, Njoku I, Hofstetter CP, Tsiouris AJ, et al. Radiographic and clinical outcome of silicate-substituted calcium phosphate (Si-CaP) Ceramic bone graft in spinal fusion procedures. Clinical Spine Surgery. 2017;30(6): E845-E52. https://doi.org/10.1097/bsd.0000000000000432

16. Ge R., Xun C., Yang J., Jia W., Li, Y. Efeito terapêutico in vivo da wollastonita e hidroxiapatita no defeito ósseo. Materiais Biomédicos. 2019;14(6):065013. https://doi.org/10.1088 /1748-605x/ab